Published in final edited form as:
Eur J Immunol. 2008 February ; 38(2): 448–458. doi:10.1002/eji.200737485.

CNS Infiltrating CD4+ T lymphocytes Contribute to Murine Spinal Nerve Transection-Induced Neuropathic Pain

Ling Cao[a,*] and **Joyce A. DeLeo**[a,b,*]

[a] Department of Anesthesiology, HB 7125, Dartmouth Hitchcock Medical Center, Lebanon, NH 03756, USA

[b] Department of Pharmacology and Toxicology, HB 7650, Dartmouth Medical School, Hanover, NH 03755, USA

Summary

We previously reported leukocytic infiltration into the lumbar spinal cord in a rodent spinal nerve L5 transection (L5Tx) neuropathic pain model. Here, we further investigated the role of infiltrating T lymphocytes in the etiology of persistent pain following L5Tx. T lymphocyte deficient nude mice showed no evident mechanical hypersensitivity after day 3 of L5Tx compared to wild type BALB/c mice. Through FACS analysis, we determined that significant leukocytic infiltration ($CD45^{hi}$) into the lumbar spinal cord peaked at day 7 post-L5Tx. These infiltrating leukocytes contained predominantly $CD4^+$ but not $CD8^+$ T lymphocytes. B lymphocytes, natural killer cells and macrophages were not detected at day 7 post-L5Tx. No differences in the activation of peripheral $CD4^+$ T lymphocytes were detected in either the spleen or lumbar lymph nodes between L5Tx and sham surgery groups. Further, CD4 KO mice displayed significantly decreased mechanical hypersensitivity after day 7 of L5Tx and adoptive transfer of $CD4^+$ leukocytes reversed this effect. Decreased immunoreactivity of glial fibrillary acidic protein observed in CD4 KO mice post-L5Tx indicated possible T lymphocyte-glial interactions. These results strongly support a contributing role of spinal cord infiltrating $CD4^+$ T lymphocytes versus peripheral $CD4^+$ T lymphocytes in the maintenance of nerve injury-induced neuropathic pain.

Keywords

$CD4^+$ T lymphocytes; Leukocyte infiltration; Nude mice; CD4 knockout mice

1. Introduction

Neuropathic pain, defined as pain initiated or caused by a primary lesion or dysfunction in the nervous system [1], is one of the most devastating forms of chronic pain. The lack of a complete understanding of its etiology thwarts the treatment and prevention. Further delineating the mechanisms leading neuropathic pain is crucial and may accelerate the design of novel, non-addictive agents. Towards this end, many rodent models of neuropathy have been developed and utilized to decipher peripheral and CNS mechanisms that give rise to long-lasting behavioral hypersensitivity, the animal correlate of painful neuropathy in humans [2]. A novel mechanistic theme has emerged in the last decade implicating a role of

*Corresponding authors: Joyce A. DeLeo, PhD, Department of Anesthesiology, HB 7125, Dartmouth Hitchcock Medical Center, Lebanon, NH 03756, USA, Tel: +1-603-650-6204; Fax: +1-603-650-8449 Joyce.A.DeLeo@Dartmouth.edu and Ling Cao, MD PhD, Department of Anesthesiology, HB 7125, Dartmouth Hitchcock Medical Center, Lebanon, NH 03756, USA, Tel: +1-603-650-6205; Fax: +1-603-650-8449 Ling.Cao@Dartmouth.edu.

central nervous system (CNS) innate and adaptive immunity in both the generation and maintenance of chronic pain syndromes [3].

Using radiation bone marrow chimeric rats, we have previously shown that spinal nerve L5 transection (L5Tx) induced significant CNS lumbar spinal cord infiltration of peripheral immune cells compared to sham surgery. These infiltrating cells were found to co-regionalize with $ED2^+$ macrophages and contained $CD3^+$ T lymphocytes [4]. Consistent with this infiltration, we have also shown increased lumbar spinal cord expression of monocyte and T lymphocyte chemoattractants, including interferon-gamma inducible protein-10 (IP-10), regulated upon activation normal T-cell expressed and secreted (RANTES), macrophage-inflammatory protein (MIP) -1α and MIP-1β, and monocyte chemoattractant protein-1 (MCP-1) at 3, 7 and 14 days following L5Tx [5]. The localized breakdown of the blood-spinal cord barrier following nerve transection [6] is thought to also facilitate leukocyte infiltration. In addition, we have demonstrated the presence of activated microglia expressing major histocompatibility class (MHC) II and the co-stimulatory molecule B7.2 (CD86) in the spinal dorsal horn following peripheral nerve injury suggesting a role of CNS adaptive immunity [7,8]. However, the specific role of these immune responses and CNS infiltrating T lymphocytes in nerve injury-induced neuropathic pain development and maintenance has not been extensively investigated.

Leukocyte infiltration into the affected peripheral nerve structures during neuropathic pain has been reported in patients suffering neuropathic pain and in the sciatic nerve chronic constriction injury (CCI) -induced animal model of neuropathic pain [9,10]. The contributing role of various types of leukocytes in pain genesis/maintenance has been demonstrated in the CCI model. Rodents with neutrophil depletion or functional T lymphocyte deficiency developed significantly reduced CCI-induced mechanical allodynia and/or thermal hyperalgesia [9,11]. The role of infiltrating leukocytes in the CCI model of neuropathic pain was further suggested by chemotactic cytokine receptor 2 (CCR2) KO mice, which exhibit a decreased recruitment of monocytes/macrophages into the dorsal root ganglia (DRG) and abrogated mechanical allodynia post-CCI [12].

In the current study, we extended our initial CNS adaptive immunity observations by using quantitative FACS analyses over a time course in the mouse neuropathy model, L5Tx; probed the differences in peripheral *vs.* infiltrating leukocytes in the same study; and addressed diverging mechanisms of initiating and maintaining nerve injury-induced behavioral hypersensitivity. Our results clearly demonstrate a role of CNS trafficking $CD4^+$ T lymphocytes in the maintenance of nerve injury – induced tactile hypersensitivity.

2. Results

2.1 Behavioral mechanical sensitivity of nude BALB/c mice post-L5Tx

To determine the role of T lymphocytes in L5Tx-induced neuropathic pain, adult T lymphocyte-deficient nude mice on BALB/c background were subjected to L5Tx or sham surgery, and then mechanical sensitivity (indicated by the 50% threshold force for paw withdrawals) was determined by the Up-Down method using von Frey filaments. All mice were baseline tested before surgery and tested again at day 1, 3, 5, 7, 11, and 14 post-surgery. No significant baseline behavioral difference between wild type (WT) and nude mice was detected. As expected, WT mice showed significant mechanical hypersensitivity throughout the observation period (up to day 14 post-L5Tx). Nude mice developed mechanical hypersensitivity day 1 post-L5Tx. However, they displayed a reduced mechanical sensitivity similar to that of sham operated animals after day 3 post-surgery (Figure 1). Two-way analysis of variance (ANOVA) revealed a statistically significant

interaction between time and surgery ($p = 0.0444$), as well as significant effects from time and surgery ($p < 0.0001$ for both).

2.2 Lumbar spinal cord infiltrating T lymphocytes post-L5Tx

To further analyze the spinal cord infiltrating T lymphocytes, we first determined the time course of leukocyte infiltration into the lumbar spinal cord via FACS analysis. We isolated total lumbar spinal cord cells 1, 3, 7 and 14 days post-L5Tx and labeled them with PE anti-mouse CD45 for flow cytometry. $CD45^{hi}$ populations were identified as the infiltrating leukocytes (Figure 2A and B). L5Tx induced a transient increase in the infiltration of peripheral leukocytes that peaked at day 7 and diminished by day 14 within both sham and L5Tx surgery groups (Figure 2C, two-way ANOVA, $p_{time} < 0.0010$). At day 7, the L5Tx group had significantly higher infiltration in both the ipsilateral (day 7 vs. days 1, 3 and 14) and contralateral (day 7 vs. day 14) sides of lumbar spinal cord, while no statistically significant increases at day 7 were seen within the sham groups. Further, no differences between ipsilateral *vs.* contralateral lumbar spinal cord within either group were observed. The infiltration appeared to be localized to the lumbar region, since no evident infiltration was observed in the remote cervical region of spinal cord in either sham or L5Tx operated mice compared to naive spinal cord (Figure 2B). Because of these findings, the following studies were focused on the lumbar spinal cord at day 7 post-injury.

To further assess the phenotype of L5Tx-induced infiltrating leukocytes, particularly the subtypes of T lymphocytes, mononuclear cells of lumbar spinal cord isolated 7 days post sham or L5Tx surgery were subjected to multiple fluorescence labeling. Due to limited cell yield from each animal and lack of significant side differences in the $CD45^{hi}$ population (Figure 2C), spinal cords from 3 or 4 animals were pooled together and not separated into ipsilateral and contralateral sides for analysis during these experiments. $CD45^{hi}$ cells were first identified (Figure 3A), and then within this population, $CD4^+$ T lymphocytes ($CD3^+CD4^+$), $CD8^+$ T lymphocytes ($CD3^+CD8^+$), B lymphocytes ($CD3^-CD19^+$), natural killer (NK) cells ($CD3^-panNK^+$), and macrophages ($CD3^-CD11b^+I\text{-}A^{d+}$) were further delineated. $CD4^+$ T lymphocytes ($CD3^+CD4^+$) were identified as the most consistent and dominant cell type within the infiltrating populations in both L5Tx and sham groups of samples from three independent experiments (Figure 3B and data not shown). $CD8^+$ T lymphocytes and other types of leukocytes were not detectable at this time point. To confirm that the identification of $CD3^+CD4^+$ T lymphocyte was specific, CD4 KO mice were subjected to sham and L5Tx surgeries and the $CD45^{hi}$ population from lumbar spinal cords 7 days post-surgery was analyzed similarly. No $CD3^+CD4^+$ population was detected from CD4 KO mice (Figure 3B right panel).

To visualize the infiltrating $CD4^+$ T lymphocytes, L5 spinal cord sections from 3 BALB/c mice at day 7 post-L5Tx were labeled with anti-CD4 mAb via fluorescence immunohistochemistry. $CD4^+$ cells with typical T lymphocyte morphology were observed mostly in the ipsilateral dorsal horn region (representative photomicrographs are shown in Figure 3C). Although some $CD4^+$ cells were also seen in the ventral horns of both ipsilateral and contralateral side of L5 spinal cord (no evident difference in numbers), no $CD4^+$ cells were detected in the contralateral side of dorsal horn following peripheral nerve injury.

2.3 Peripheral $CD4^+$ T lymphocyte responses

$CD4^+$ T lymphocytes in the spleen and local draining lumbar lymph nodes (LNs) in sham and L5Tx mice were analyzed to determine whether there were any associated changes in the periphery. Total numbers of splenocytes, but not splenic $CD4^+$ T lymphocytes, were increased with time post-L5Tx or sham surgery with the peak level at day 3 (Figure 4A and B, in A two-way ANOVA $p_{time} = 0.0019$). The percentage of $CD4^+$ T lymphocytes in

lumbar LNs significantly increased and peaked at day 7 post both surgeries (Figure 4C, two-way ANOVA $p_{time} = 0.0295$). Further, in both spleen and lumbar LNs, a slight but significant activation of $CD4^+$ T lymphocytes was detected after both surgeries as indicated by increased surface expression of CD69 and CD154 (Figure 4D and 4E, two-way ANOVA, in D $p_{time} = 0.0006$, and in E $p_{time} = 0.0091$) for splenic cells, and of $CD45RB^{lo}$ for both splenic (data not shown, two-way ANOVA, $p_{time} = 0.0003$) and LNs cells (Figure 4F, two-way ANOVA, $p_{time} = 0.0484$). However, no differences between L5Tx and sham surgery were identified in all cases. Additionally, no differences between L5Tx and sham surgeries in the percentages of other subtypes of leukocytes [$CD8^+$ T lymphocytes ($CD3^+CD8^+$), B lymphocytes ($CD3^-CD19^+$), natural killer (NK) cells ($CD3^-panNK^+$), and macrophages ($CD3^-CD11b^+I\text{-}A^{d+}$)] were detected in the spleens at day 7 post-surgery (data not shown).

2.4 Behavioral mechanical sensitivity of CD4 KO BALB/c mice post-L5Tx

To further determine the role of $CD4^+$ T lymphocytes in L5Tx-induced neuropathic pain, adult CD4 KO BALB/c mice, which lack functional $CD4^+$ T lymphocytes, were subjected to L5Tx or sham surgery. All mice were baseline tested before surgery and repeatedly tested at day 1, 3, 5, 7, 11, 14, 18 and 21 post-surgery for their mechanical sensitivity using the Up-Down method as described in section 2.1. No significant baseline behavioral difference between WT and CD4 KO mice was detected. Although L5Tx induced similar mechanical hypersensitivity in both CD4 KO mice and WT mice initially (day 0 to 5), CD4 KO mice displayed significant reduced mechanical hypersensitivity at a later phase (after day 7) post-nerve injury (Figure 5A; Two-way ANOVA analysis: $p_{time \times surgery} < 0.0001$; $p_{time} < 0.0001$, and $p_{surgery} < 0.0001$). CD4 KO mice adoptively transferred with 3×10^6 negatively selected $CD4^+$ leukocytes showed heightened mechanical sensitivity compared to CD4 KO mice without transfer (Figure 5B; Two-way ANOVA analysis: $p_{time\ x\ treatment} < 0.0206$; $p_{time} < 0.0271$, and $p_{treatment} < 0.0001$). Similarly, CD4 KO mice receiving 20×10^6 of mixed splenic and lymph node leukocytes also showed increased behavioral sensitivity compared to CD4 KO mice without transfer (data not shown).

2.5 Lumbar spinal cord glial responses post-L5Tx

It has been shown that glial activation post-L5Tx plays a key role in L5Tx-induced behavioral hypersensitivity [3]. Therefore, we examined astocytic and microglial responses at day 7 post-L5Tx in both WT and CD4 KO mice via immunohistochemistry. Naïve, L5Tx or sham operated WT and CD4 KO mice were used (n = 2 for both WT and CD4 KO naive groups, and sham-operated CD4 KO group; n = 3 for both WT and CD4 KO L5Tx groups, and sham-operated WT group). Anti-glial fibrillary acidic protein (GFAP) and CD11b antibodies were used for labeling astrocytes and microglia, respectively. We focused on the ipsilateral dorsal horn region, which previously showed consistent and significant increase in the immunoreactivity of both GFAP and CD11b post-L5Tx [13]. As predicted, L5Tx induced significantly increased immunoreactivity of both GFAP and CD11b in the ipsilateral L5 dorsal horn region in the WT BALB/c mice (Figure 6A and B top panel). Similarly, significantly increased expression of CD11b in CD4 KO mice was also observed, while no significant increase in GFAP expression was detected in CD4 KO mice at the same time (Figure 6A and B lower panel).

3. Discussion

It has been clearly demonstrated that nerve injury-induced behavioral hypersensitivity can be divided into at least two phases: an initiation phase (from day 0 to ~day 5) and a maintenance phase (after ~day 5) based on the pattern of nociceptive behaviors and the animals' responses to selective drug treatments [14–16]. The initiation phase may be more reflective of an acute pain mechanism that transfers to a chronic phase if unabated. Our

results demonstrate a contributing role of CNS infiltrating $CD4^+$ T lymphocytes in maintaining tactile hypersensitivity following peripheral nerve injury. No differences in peripheral $CD4^+$ T lymphocytes responses between L5Tx and sham surgery groups were observed. Our previous studies of MHC II KO mice, which have decreased mature $CD4^+$ T lymphocytes and showed reduced L5Tx-induced hypersensitivity [8], support the current findings.

$CD4^+$ T lymphocytes continuously circulate through the CNS to provide immunological surveillance [17]. However, $CD4^+$ T lymphocytes are also linked to various CNS pathological conditions. $CD4^+$ T lymphocyte-mediated autoimmune responses are vital in the pathogenesis of multiple sclerosis and to some extent, Alzheimer's disease [18,19]. Alternatively, CNS infiltrating activated $CD4^+$ T lymphocytes promote facial motoneuron survival following axotomy injury [20], possibly via their brain-derived neurotrophic factor (BDNF) production [21]. The report that intraperitoneal injection of *in vitro* driven type 1 helper T (Th1) lymphocytes induced nociceptive hypersensitivity post-CCI in athymic nude rats (rnu−/−), while type 2 helper T lymphocytes prevented the behavioral hypersensitivity in the heterozygous rnu+/− rats [9], provided initial evidence of the involvement of $CD4^+$ T lymphocytes in neuropathic pain. We and others have also previously detected $CD4^+$ cells in the lumbar spinal cord or DRG in animal models of neuropathic pain, which were thought to be mostly CD4 expressing macrophages/microglia [8,22]. In the current study, we clearly detected $CD3^+CD4^+$ T lymphocytes in the lumbar spinal cord post-L5Tx at day 7 post-L5Tx via both FACS and immunohistochemistry. Our results from CD4 KO mice further confirm the contributing role of $CD4^+$ T lymphocytes in the later phase of neuropathic pain progression. Interestingly, a recent report suggests that the presence of $CD4^+$ T lymphocytes in the gut exhibits an antinociceptive effect in a mouse model of visceral pain, possibly through their release of endorphins [23]. Together with our current findings, these results highlight a complex role of the immune system, particularly $CD4^+$ T lymphocytes, in pain modulation. Additionally, we had previously demonstrated macrophage-like cell infiltration at early time points after peripheral nerve injury using radiation bone marrow chimeric rats [4]. The disparity between that and our current study may relate to the differences in species (rats *vs.* mouse) and method of detection (immunohistochemistry *vs.* FACS).

Multiple factors may be involved in regulating migration of $CD4^+$ T lymphocytes into the CNS and their localization within the CNS. Differential expression in cytokine/chemokine receptor and/or adhesion molecules on infiltrating $CD4^+$ T lymphocytes determines their ability to migrate into the CNS and their specific interactions with CNS resident cells [24,25]. Increased lumbar spinal cord IP-10 expression post-L5Tx [5] would suggest a Th1 phenotype of the observed CNS infiltrating $CD4^+$ T lymphocytes, which is supported by the fact that adoptive transfer of Th1 cells produced hypersensitivity in nude rats following CCI [9]. High concentrations of extracellular glutamate have been known to induce neuronal damage and central nociceptive sensitization. Expression of both constitutive and inducible metabotropic glutamate receptors by T lymphocytes may promote neuron-T lymphocyte interactions in the CNS [26]. Antigen specific interactions between $CD4^+$ T lymphocytes and activated resident microglia may induce the formation of CNS immunosynapses [27] and further modulate T lymphocyte-mediated CNS adaptive immunity.

The specific mechanisms of how infiltrating leukocytes mediate neuropathic pain are unknown. We suspect that the CNS local environment (cellular and soluble factors, such as CNS glia and their secreted products) is actively involved in the actions of infiltrating $CD4^+$ T lymphocytes and the resulting sequelae. The involvement of local factors also explains the long-lasting pro-nociceptive effects resulting from the relatively temporary infiltration of $CD4^+$ T lymphocytes into the spinal cord. Our immunohistochemical study illustrated that the majority of infiltrating $CD4^+$ T lymphocytes were observed in the dorsal horn region of

the ipsilateral spinal cord, which is also the area showing the most significant activation of astrocytes and microglial post-L5Tx [13]. It is reasonable to hypothesize that infiltrating $CD4^+$ T lymphocytes interact with CNS local glia and induce further glial responses, such as production of proinflammatory mediators by glial cells. It has been well-established that nitric oxide (NO), prostaglandin E_2 (PGE_2), the proinflammatory cytokines IL-1β, IL-6 and TNFα, and chemokines can be linked to spinal sensitization and the pathogenesis of persistent pain state [28].

A recent publication by Clark *et. al.* [29] reported that peripheral nerve injury led to the expression of the lysosomal cysteine protease cathepsin S (CatS) in activated microglia in the ispilateral dorsal horn, with expression peaking at day 7 and remaining high on day 14. CatS was shown to further release soluble chemokine fractalkine, which in turn, initiated downstream proinflammatory responses. Since the maximal $CD4^+$ T lymphocyte infiltration was observed at day 7, it is likely that $CD4^+$ T lymphocyte-microglial interaction results in the microglial secretion of CatS and further pro-inflammatory responses in maintaining neuropathic behaviors. Future studies will be conducted to test this pathway.

The lack of a detectable significant difference in microglial CD11b expression between WT and CD4 KO mice only indicates that changes in multiple microglial factors (other than CD11b) may exist from $CD4^+$ T lymphocytes-microglial interaction, e.g. Iba-1 or MHC Class II expression. The observed differential immunoreactivity in GFAP between WT and CD4 KO mice is consistent with the concept that astrocytes have been associated with the maintenance of L5Tx-induced neuropathic pain [3]. Our previous observations of increases in the co-stimulatory molecule B7.2 and MHC II in the lumbar spinal cord post-L5Tx and significantly decreased pain behaviors post-L5Tx in MHC II KO mice [4,7,8] support the involvement of T lymphocyte-mediated adaptive immunity in pain.

Interestingly, Schwartz *et. al.* group have reported that passive administration of T lymphocytes specific to self antigens, at selected times, could promote the recovery from both post partial optic nerve crush injury [30] and post incomplete spinal cord injury [31] in rodents supporting the concept of protective autoimmunity. Whether the observed $CD4^+$ T lymphocytes in the spinal cord post-L5Tx respond to specific CNS antigen(s) and whether this possible T cell specificity plays a role in maintaining behavioral hypersensitivity requires further investigation. Alternatively, we hypothesize that the T lymphocyte infiltration following nerve injury is a protective mechanism to promote neuronal survival but may also concomitantly induce neuronal sensitization.

The finding that CD4 KO mice did not display complete reversal of L5Tx-induced behavioral hypersensitivity indicates that L5Tx induced neuropathic pain is partially modulated by $CD4^+$ T lymphocytes. It has been established that activation of both astrocytes and microglia plays crucial roles in the etiology of neuropathic pain following nerve injury [3]. The finding that the numbers of both astrocytes and microglia in adult nude mice (13-week) were significantly reduced (31% and 33% respectively) compared to normal BALB/c mice in the CNS [32] may explain the further reduction of mechanical hypersensitivity in nude mice compared to CD4 KO mice post-L5Tx and warrants further investigation. It is also possible that other non-immunological mutations in the nude mouse could be responsible for these differential changes in mechanical hypersensitivity. However, no other pain sensation/transmission related mutations (other than the difference in glial numbers mentioned above) in nude mice have been detected so far.

Finally, current treatments for neuropathic pain are not universally effective and are often associated with a myriad of side effects such as physical dependence, hyperalgesia, tolerance, and sedation. Innovative approaches to reduce $CD4^+$ T lymphocyte infiltration by

chemokine/cytokine inhibition or regulating interactions between infiltrating $CD4^+$ T lymphocytes and their CNS targets may reduce $CD4^+$ T lymphocyte-mediated CNS responses after nerve injury, and thus can be used in chronic neuropathic pain management.

4. Materials and methods

4.1 Animals

Male BALB/c mice (7–8 week old) were purchased from Charles River (Wilmington, MA) or National Cancer Institute (NCI, Frederick, MD). Male nude BALB/c mice (7–8 week old) were purchased from NCI. These animals were allowed to habituate to the animal facility for at least 1 week before being used in experiments. Breeding pairs for CD4 KO mice were obtained from Dr. William T. Lee of Wadsworth Center, New York State Department of Health and maintained in the Dartmouth-Hitchcock Medical Center animal facility. Dr. Lee originally obtained homozygous BALB/c CD4 KO mice from Dr. Steve Reiner at the University of Pennsylvania who generated these mice from CD4 KO mice with B6/129 background [33] (Mice from the fifth backcross were used in this original publication). In Dr. Lee's laboratory, only occasionally (less than three times), BALB/c CD4 KO mice were backcrossed to BALB/c mice when the mouse line was getting low, and then they were inter-crossed regularly. The mouse line is randomly screened by PCR and FACS of peripheral blood. All mice used in the current experiment are from the first and second generations of breeding since the breeding pairs arrived at Dartmouth. Both male and female CD4 KO mice were used due to limited production of male mice. No significant behavioral differences in mechanical sensitivity were observed between sexes (data not shown). T lymphocyte deficiency in nude mice and CD4 deficiency in CD4 KO mice were further confirmed at the end of experiments through FACS analysis of blood leukocyte CD3 and CD4 expression, respectively. All mice were group-housed (3–4 per cage) with food and water *ad libitum*. All animals were maintained on a 12-h light/dark cycle. Mice were 8–9 week old when used and about 21–25 g per mouse. The Institutional Animal Care and Use Committee (IACUC) at Dartmouth College approved all experimental procedures.

4.2 Spinal nerve L5 transection (L5Tx)

Surgery was conducted following previously published procedure [34]. Briefly, mice were anesthetized by inhalation of halothane (4% for induction and 2% for maintenance) in 100% O_2. To expose the spinal nerve L5, a 1–2 cm skin incision overlying the L4-S1 section was made and the muscle tissue was separated and retracted from the left superior articular processes and the transverse process. The L6 transverse process was cleaned and the spinal nerve L4 and L5 were exposed. The L5 spinal nerve was gently separated from the L4 spinal nerve, lifted slightly, and transected with removal of a 1–2 mm segment of nerve (to prevent reconnection). The wound was irrigated with sterile saline, and closed using a 6-0 silk suture for the fascia and a 3-0 polyester suture for skin. Sham surgery was performed identically except that the L5 spinal nerve was not manipulated in any way following the partial laminectomy. Mice were randomly selected into either sham or L5Tx groups.

4.3 Assessment of mechanical sensitivity

The tactile sensitivity response was measured as the direct pressure stimulus required to elicit foot-withdrawal in non-restrained conditions. All tests were conducted in the morning between 8:30–11:30 AM. Animals were habituated to the testing apparatus for at least 40 min before testing. Each animal was subjected to the stimulation of a series of von Frey filaments (Stoelting, Wood Dale, IL) ranging from 0.008 g to 2 g (log force 1.65, 2.36, 2.44, 2.83, 3.22, 3.84, 4.08, 4.17 and 4.31) using the Up-Down paradigm (detailed in [35]). The selected von Frey filament was pressed against the plantar surface of the ipsilateral (side of surgery) hind paw to the point of 30^o bending for 3 sec. Paw withdrawal response was

considered as the positive response. The fifty percent threshold force needed for paw withdrawal was calculated for each mouse and used to represent the mechanical sensitivity of this animal. For each experiment, animals were previously baseline tested before L5Tx and tested at selected times post-surgery. The person performing the behavioral tests was blinded to the experimental groups.

4.4 Sample preparation for flow cytometry

Mice were euthanized by CO_2 and transcardially perfused with 0.1M phosphate-buffered saline (PBS, pH 7.4; between 50–100 ml per mouse), and then the spinal cords, spleens and lumbar local lymph nodes were harvested. The ipsilateral and contralateral (relative to the injury) portions of the lumbar region of each spinal cord were further dissected in selected experiments. In some experiments (as described in the Results), a remote region of spinal cord (cervical section of spinal cord) was also collected.

To obtain total cells from spinal cord sections, spleen and lymph nodes, each tissue was homogenized and filtered through a 70 micron cell strainer (BD Biosciences, San Diego, CA). After cells were washed with PBS, they were ready for staining. Red blood cells in splenocytes were lysed with a lysing buffer containing ammonium chloride. Total splenocyte numbers were then determined using a hemacytometer (Fisher Scientific, Hampton, NH) with trypan blue (Sigma, St Louis, MO) before staining for FACS. All spinal cord and lymph node cells were collected and used for staining.

To obtain mononuclear cells from spinal cord tissue, discontinuous Percoll gradients were used following a published method [36]. Due to the limited numbers of mononuclear cells recovered from each tissue piece from a single animal, total cell suspensions prepared (as described above) from 3–4 mice were pooled together for processing. Briefly, after washing, the cell pellet was resuspended in 8 ml of 40% Percoll [100% PerColl was prepared by mixing 1 part 10x PBS with 9 parts Percoll solution (Amersham, Piscataway, NJ)] in 15 ml conical tubes, and then centrifuged at 800 ×g, 22 ^{o}C for 30 min without breaking. After removal of the top layer of myelin debris and supernatant, the cell pellet was resuspended in 8 ml of 70% Percoll and centrifuged again as above. The resulting mononuclear cell fraction (top layer) was carefully collected and cells were further washed twice with PBS containing 3% fetal bovine serum (FBS, HyClone, Logan, UT) followed by PBS. Total mononuclear cell number was determined using a hemacytometer with trypan blue before staining for FACS.

4.5 Flow cytometry

Following the final wash with PBS in the cell preparation above, cells were resuspended in staining buffer (2% FBS and 0.09% NaN_3 in PBS) containing anti-mouse-CD16/CD32 (1μg/50 μl/tube), and incubated on ice for 30 min to block Fc receptors. Then, combinations of 2–5 fluorescent-labeled or biotinylated mAbs were added into each tube and cells were incubated on ice for another 30 min. After washing twice with PBS, if a biotinylated primary antibody was used, the secondary reagent streptavidin-perCP (BD Biosciences) was added and cells were again incubated on ice for 30 min, and then washed twice with PBS. All stained cells were finally resuspended in 1% formaldehyde/PBS and stored at 4 ^{o}C until analysis. The combinations of primary mAbs used are shown in detail in Table 1. After the completion of staining, a total of 100,000 events (for total cells from lumbar spinal cord), up to 10,000 events (for spinal cord mononuclear cells and cells from lumbar lymph nodes) or 30,000 events (for splenocytes) from each sample were analyzed using a FACSCanto flow cytometer with Cell Quest software (BD Biosciences). Non-stained cells from the same tissue with the same preparation were included in each run as the negative control and reference for data analysis.

4.6 Leukocyte isolation and mouse adoptive transfer

Splenocytes and lymph node (axillary and inguinal LNs) cells were aseptically isolated as described above in section 4.4 from 7-week old female BALB/c mice. All cells were pooled together in sterile Dulbecco's Phosphate Buffered Saline (DPBS) containing 2% FBS after final wash at 1×10^{8}/ml. One portion of cells was kept on ice for later use. The remaining cells were subjected to further $CD4^+$ cell isolation by Robosep automated cell separator using EasySep negative selection mouse $CD4^+$ T cell enrichment kit (StemCell Technologies, Vancouver, BC, Canada). Collected $CD4^+$ cells and non-separated total leukocytes were resuspended in sterile PBS for adoptive transfer. Six to eight week old CD4 KO mice (male and female) were used as recipient mice. $CD4^+$ cells were intravenously (i.v.) injected at 3×10^{6}/200 μl per mouse, and total leukocytes were i.v. injected at 20×10^{6}/200 μl per mouse. Non-injected CD4 KO mice were served as controls. $CD4^+$ T cells contents in both types of injected cells were determined by FACS using PE-Cy7-anti-CD3 and FITC-anti-CD4 mAbs (BD Biosciences). $CD4^+$ cell and $CD3^+CD4^+$ cell contents were at 34.31% and 24.93% in total leukocytes, respectively. $CD4^+$ cell and $CD3^+CD4^+$ cell contents were at 96.58% and 74.80% in isolated $CD4^+$ cells, respectively. Mice underwent L5Tx surgery on day 8 post-transfer and were monitored for their mechanical sensitivity up to day 14 post-surgery as described earlier. One or two mice from each transfer group were sampled on the day of surgery and upon the completion of behavioral testing to verify the positive existence of $CD4^+$ cells in peripheral blood, LNs and spleen via FACS.

4.7 Immunohistochemistry

WT and CD4 KO mice subjected to L5Tx or sham surgery were deeply anesthetized by inhalation of isoflurane (4%) in 100% O_2. Mice were transcardially perfused with 0.1 M PBS (pH 7.4, ~100 ml per mouse) followed by 4% formaldehyde in 0.1M PBS (between 100–150 ml per mouse). The L5 segment of lumbar spinal cord was harvested and cryo-protected in 30% sucrose for at least 72 hr at 4 °C. Tissue was then freeze-mounted in OCT embedding medium (Sakura Finetek, Torrance, CA) on cork blocks for cryostat sectioning. Immunohistochemistry was performed on 20μm L5 spinal cord sections mounted on Superfrost/Plus microscope slides (Fisher Scientific, Pittsburg, PA).

Fluorescent immunohistochemistry for CD4 was conducted as previously described [4]. FITC labeled anti-mouse CD4 (BD Biosciences) was used at a 1:50 dilution. Slices were examined using an Olympus fluorescence microscope (U-ULH) (Olympus Optical CO., LTD., Japan) with an Olympus Q-FIRE camera. Light level immunohistochemistry for glial cells was conducted using an avidin-biotinylated enzyme complex technique (Vextor Laboratories, Burlingame, CA) with 3, 3′-Diaminobenzidine tetrahydrochloride (DAB) (Sigma) as the substrate, as previously described [37]. Abs for CD11b (for microglia, from Serotec, Raleigh, NC) and glial fibrillary acidic protein (GFAP, for astrocytes, from DAKO UK LTD., UK) were used at 1:100 and 1:5,000 dilution respectively. Images of all sections were taken via an Olympus fluorescence microscope (U-ULH) (Olympus Optical CO.) with an Olympus Q-FIRE camera and then analyzed with SigmaScan Pro 5 (Aspire Software International, Ashburn, VA) for the total number of pixels in the ipsilateral dorsal horn region. Average numbers of pixels from 3 to 4 slices of each animal was used to represent the immunoreactivity of each animal.

4.8 Statistical analysis

All data were graphed with SigmaPlot 9.0 (Systat Software, Inc. San Jose, CA) and analyzed using GraphPad Prism 4 (GraphPad Software Inc. San Diego, CA). For comparison of mechanical sensitivity and cellular phenotypes, appropriate two-way analysis of variance (ANOVA) with time and surgery as factors was performed followed by Bonferroni *Post hoc*

analysis. All data are presented as mean ± SEM when applicable. $p < 0.05$ was considered as statistically significant.

Acknowledgments

The authors would like to thank Dr. Alice Givan and Gary Ward in the Englert Cell Analysis Laboratory in the Dartmouth Medical School for their help in flow cytometric analysis. The authors thank Dr. Jacqueline. Y. Smith and Ms. Kathy Smith in the Immune Monitoring Laboratory in the Dartmouth Medical School for conducting $CD4^+$ cell isolation using Robosep automated cell separator. The authors are grateful for the technical help from Ms. Nancy Nutile-McMenemy in Dr. Joyce DeLeo's Laboratory. The authors also thank Dr William T. Lee from the Wadsworth Center, New York State Department of Health (Albany, NY) for providing CD4 KO BALB/c mice breeding pairs. This work was supported by 5 RO1 DA11276 (NIDA) and T32 AI 07363-15 grants from NIH.

List of abbreviations

L5Tx	Spinal nerve L5 transection
IP-10	Interferon-gamma inducible protein-10
DRG	Dorsal root ganglia
CCI	Chronic constriction injury
CNS	Central nervous system
BDNF	Brain-derived neurotrophic factor
GFAP	glial fibrillary acidic protein
CatS	cathepsin S

References

1. Backonja MM. Defining neuropathic pain. Anesth Analg. 2003; 97:785–790. [PubMed: 12933403]
2. Wang LX, Wang ZJ. Animal and cellular models of chronic pain. Adv Drug Deliv Rev. 2003; 55:949–965. [PubMed: 12935939]
3. DeLeo JA, Tanga FY, Tawfik VL. Neuroimmune activation and neuroinflammation in chronic pain and opioid tolerance/hyperalgesia. Neuroscientist. 2004; 10:40–52. [PubMed: 14987447]
4. Sweitzer SM, Hickey WF, Rutkowski MD, Pahl JL, DeLeo JA. Focal peripheral nerve injury induces leukocyte trafficking into the central nervous system: potential relationship to neuropathic pain. Pain. 2002; 100:163–170. [PubMed: 12435469]
5. DeLeo, JA.; Winkelstein, BA.; Rutkowski, MD. Society for Neuroscience 32nd Annual Meeting. Orlando, FL: Poster presentation; 2002. The modulatory role of spinal chemokine activation in neuropathic pain.
6. Gordh T, Chu H, Sharma HS. Spinal nerve lesion alters blood-spinal cord barrier function and activates astrocytes in the rat. Pain. 2006; 124:211–221. [PubMed: 16806707]
7. Rutkowski MD, Lambert F, Raghavendra V, DeLeo JA. Presence of spinal B7.2 (CD86) but not B7.1 (CD80) co-stimulatory molecules following peripheral nerve injury: role of nondestructive immunity in neuropathic pain. J Neuroimmunol. 2004; 146:94–98. [PubMed: 14698851]
8. Sweitzer SM, White KA, Dutta C, DeLeo JA. The differential role of spinal MHC class II and cellular adhesion molecules in peripheral inflammatory versus neuropathic pain in rodents. J Neuroimmunol. 2002; 125:82–93. [PubMed: 11960644]
9. Moalem G, Xu K, Yu L. T lymphocytes play a role in neuropathic pain following peripheral nerve injury in rats. Neuroscience. 2004; 129:767–777. [PubMed: 15541898]
10. Hu P, McLachlan EM. Macrophage and lymphocyte invasion of dorsal root ganglia after peripheral nerve lesions in the rat. Neuroscience. 2002; 112:23–38. [PubMed: 12044469]
11. Perkins NM, Tracey DJ. Hyperalgesia due to nerve injury: role of neutrophils. Neuroscience. 2000; 101:745–757. [PubMed: 11113323]

12. Abbadie C, Lindia JA, Cumiskey AM, Peterson LB, Mudgett JS, Bayne EK, DeMartino JA, MacIntyre DE, Forrest MJ. Impaired neuropathic pain responses in mice lacking the chemokine receptor CCR2. Proc Natl Acad Sci U S A. 2003; 100:7947–7952. [PubMed: 12808141]
13. Colburn RW, Rickman AJ, DeLeo JA. The effect of site and type of nerve injury on spinal glial activation and neuropathic pain behavior. Exp Neurol. 1999; 157:289–304. [PubMed: 10364441]
14. Raghavendra V, Tanga F, DeLeo JA. Inhibition of microglial activation attenuates the development but not existing hypersensitivity in a rat model of neuropathy. J Pharmacol Exp Ther. 2003; 306:624–630. [PubMed: 12734393]
15. Wang Z, Gardell LR, Ossipov MH, Vanderah TW, Brennan MB, Hochgeschwender U, Hruby VJ, Malan TP Jr, Lai J, Porreca F. Pronociceptive actions of dynorphin maintain chronic neuropathic pain. J Neurosci. 2001; 21:1779–1786. [PubMed: 11222667]
16. Burgess SE, Gardell LR, Ossipov MH, Malan TP Jr, Vanderah TW, Lai J, Porreca F. Time-dependent descending facilitation from the rostral ventromedial medulla maintains, but does not initiate, neuropathic pain. J Neurosci. 2002; 22:5129–5136. [PubMed: 12077208]
17. Hickey WF. Basic principles of immunological surveillance of the normal central nervous system. Glia. 2001; 36:118–124. [PubMed: 11596120]
18. Delgado S, Sheremata WA. The role of CD4+ T-cells in the development of MS. Neurol Res. 2006; 28:245–249. [PubMed: 16687048]
19. Town T, Tan J, Flavell RA, Mullan M. T-cells in Alzheimer's disease. Neuromolecular Med. 2005; 7:255–264. [PubMed: 16247185]
20. Jones KJ, Serpe CJ, Byram SC, Deboy CA, Sanders VM. Role of the immune system in the maintenance of mouse facial motoneuron viability after nerve injury. Brain Behav Immun. 2005; 19:12–19. [PubMed: 15581733]
21. Serpe CJ, Byram SC, Sanders VM, Jones KJ. Brain-derived neurotrophic factor supports facial motoneuron survival after facial nerve transection in immunodeficient mice. Brain Behav Immun. 2005; 19:173–180. [PubMed: 15664790]
22. Hu P, Bembrick AL, Keay KA, McLachlan EM. Immune cell involvement in dorsal root ganglia and spinal cord after chronic constriction or transection of the rat sciatic nerve. Brain Behav Immun. 2006
23. Verma-Gandhu M, Bercik P, Motomura Y, Verdu EF, Khan WI, Blennerhassett PA, Wang L, El-Sharkawy RT, Collins SM. CD4+ T-cell modulation of visceral nociception in mice. Gastroenterology. 2006; 130:1721–1728. [PubMed: 16697736]
24. Moalem G, Leibowitz-Amit R, Yoles E, Mor F, Cohen IR, Schwartz M. Autoimmune T cells protect neurons from secondary degeneration after central nervous system axotomy. Nat Med. 1999; 5:49–55. [PubMed: 9883839]
25. Jones TB, Hart RP, Popovich PG. Molecular control of physiological and pathological T-cell recruitment after mouse spinal cord injury. J Neurosci. 2005; 25:6576–6583. [PubMed: 16014718]
26. Pacheco R, Gallart T, Lluis C, Franco R. Role of glutamate on T-cell mediated immunity. J Neuroimmunol. 2007; 185:9–19. [PubMed: 17303252]
27. Barcia C, Thomas CE, Curtin JF, King GD, Wawrowsky K, Candolfi M, Xiong WD, Liu C, Kroeger K, Boyer O, Kupiec-Weglinski J, Klatzmann D, Castro MG, Lowenstein PR. In vivo mature immunological synapses forming SMACs mediate clearance of virally infected astrocytes from the brain. J Exp Med. 2006; 203:2095–2107. [PubMed: 16923851]
28. Moalem G, Tracey DJ. Immune and inflammatory mechanisms in neuropathic pain. Brain Res Brain Res Rev. 2005
29. Clark AK, Yip PK, Grist J, Gentry C, Staniland AA, Marchand F, Dehvari M, Wotherspoon G, Winter J, Ullah J, Bevan S, Malcangio M. Inhibition of spinal microglial cathepsin S for the reversal of neuropathic pain. Proc Natl Acad Sci U S A. 2007; 104:10655–10660. [PubMed: 17551020]
30. Schwartz M, Moalem G, Leibowitz-Amit R, Cohen IR. Innate and adaptive immune responses can be beneficial for CNS repair. Trends Neurosci. 1999; 22:295–299. [PubMed: 10370250]
31. Hauben E, Agranov E, Gothilf A, Nevo U, Cohen A, Smirnov I, Steinman L, Schwartz M. Posttraumatic therapeutic vaccination with modified myelin self-antigen prevents complete

paralysis while avoiding autoimmune disease. J Clin Invest. 2001; 108:591–599. [PubMed: 11518733]

32. Htain WW, Leong SK, Ling EA. A qualitative and quantitative study of the glial cells in normal and athymic mice. Glia. 1995; 15:11–21. [PubMed: 8847097]
33. Brown DR, Moskowitz NH, Killeen N, Reiner SL. A role for CD4 in peripheral T cell differentiation. J Exp Med. 1997; 186:101–107. [PubMed: 9207001]
34. Tanga FY, Nutile-McMenemy N, DeLeo JA. The CNS role of Toll-like receptor 4 in innate neuroimmunity and painful neuropathy. Proc Natl Acad Sci U S A. 2005; 102:5856–5861. [PubMed: 15809417]
35. Chaplan SR, Bach FW, Pogrel JW, Chung JM, Yaksh TL. Quantitative assessment of tactile allodynia in the rat paw. J Neurosci Methods. 1994; 53:55–63. [PubMed: 7990513]
36. Ponomarev ED, Novikova M, Yassai M, Szczepanik M, Gorski J, Dittel BN. Gamma delta T cell regulation of IFN-gamma production by central nervous system-infiltrating encephalitogenic T cells: correlation with recovery from experimental autoimmune encephalomyelitis. J Immunol. 2004; 173:1587–1595. [PubMed: 15265886]
37. Colburn RW, DeLeo JA, Rickman AJ, Yeager MP, Kwon P, Hickey WF. Dissociation of microglial activation and neuropathic pain behaviors following peripheral nerve injury in the rat. J Neuroimmunol. 1997; 79:163–175. [PubMed: 9394789]

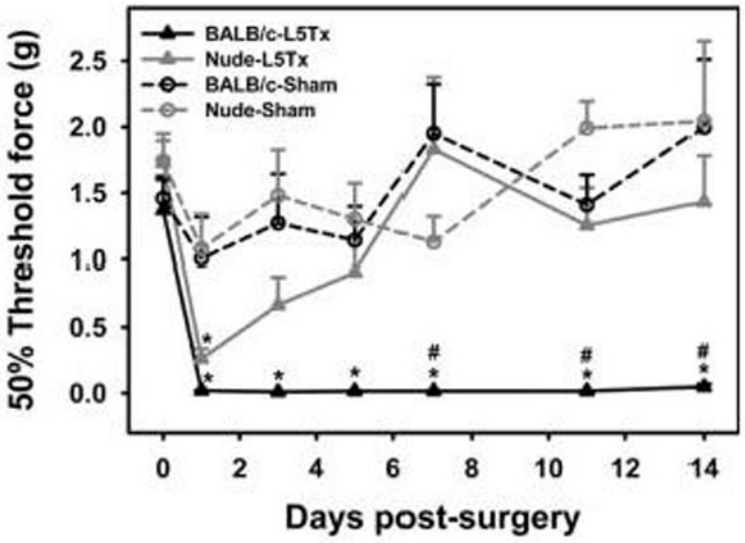

Figure 1. Mechanical sensitivity of nude/BALB/c mice post-L5Tx or sham surgery

Adult male nude/BALB/c mice and BALB/c wild type controls were subjected to L5Tx or sham surgery. Mechanical sensitivity was tested with von Frey filaments using the Up-Down method before and after surgery. Mechanical sensitivity was presented as the 50% threshold force for each animal (n = 8, mean ± SEM). * indicates significant differences between L5Tx and sham operated mice within nude or wild type groups ($p < 0.05$). ± indicates significant differences between nude and wild type mice subjected to the same surgery ($p < 0.05$).

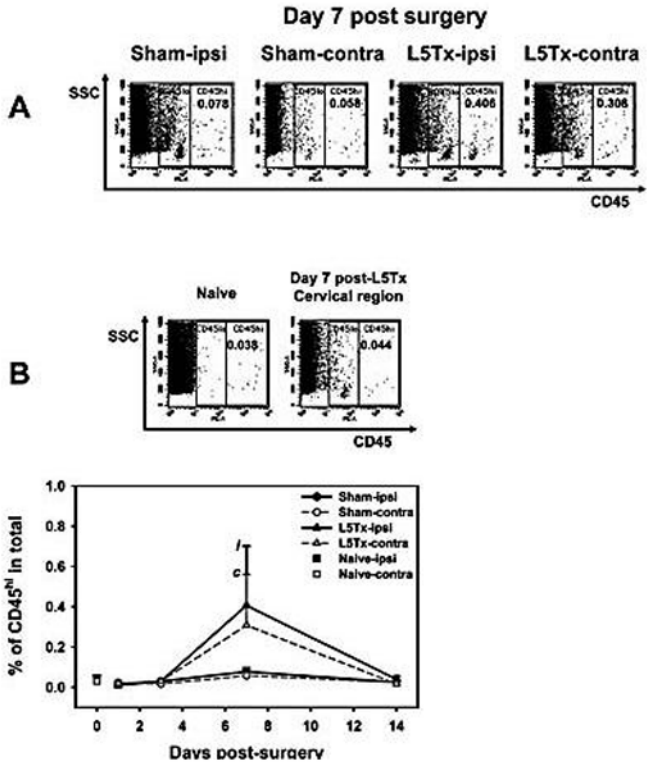

Figure 2. Time course of leukocyte infiltration into the lumbar spinal cord post-L5Tx or sham surgery in BALB/c mice

Total lumbar spinal cord cells (from both ipsilateral and contralateral sides) and cells from the cervical region of spinal cord were isolated and labeled with PE-anti-mouse CD45 mAb at day 1, 3, 7 and 14 post sham or L5Tx surgery in adult male BALB/c mice. Representative side scatter (SSC) *vs.* CD45 plots for total events collected from ipsilateral (ipsi) or contralateral (contra) lumbar spinal cords at day 7 post sham or L5Tx operation (A), naive lumbar spinal cord tissue (left panel in B), and the cervical region of spinal cord day 7 post-L5Tx (right panel in B) are presented. $CD45^{lo}$ and $CD45^{hi}$ indicate populations expressing low and high levels of CD45 respectively. Numbers in the $CD45^{hi}$ region is the average percentage of $CD45^{hi}$ population within total events analyzed (n = 2–5 per group). Time course of CD45hi expression is summarized in C and data are presented as mean ± SEM. "*i*" indicates significant differences between day 7 and day 1, 3 and 14 within ipsilateral L5Tx groups ($p < 0.05$); and "*c*" indicates significant difference between day 7 and day 14 within contralateral L5Tx groups ($p < 0.05$)

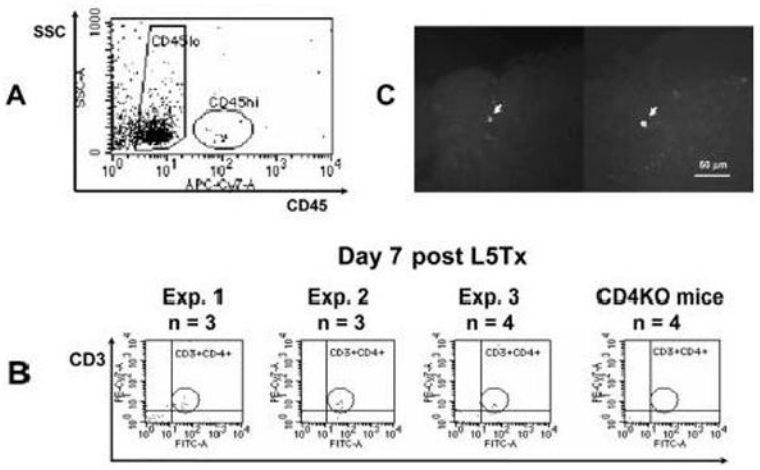

Figure 3. Phenotype of lumbar spinal cord infiltrating T lymphocytes 7 days post-L5Tx in BALB/c mice

Mononuclear cells were isolated from pooled lumbar spinal cord tissue (3 or 4 mice per group) at day 7 post sham or L5Tx surgery in adult male BALB/c mice. $CD45^{hi}$ population was first identified as shown in A, and then was analyzed in CD3 *vs*. CD4 dot plots. Results from three independent experiments are presented in B ("n" indicates numbers of animal used for each group; circles indicates $CD3^+CD4^+$ population). Similar samples were also obtained from CD4KO mice that underwent L5Tx to ensure the specific identification of $CD3^+CD4^+$ T lymphocytes (far right panel in B). Fluorescent immunohistochemical staining for CD4 was performed in the L5 lumbar spinal cord of mice 7 days post-L5Tx. $CD4^+$ cells with typical T lymphocyte morphology were identified mostly in the ipsilateral dorsal horn region. Representative photomicrographs of $CD4^+$ T lymphocytes in the ipsilateral dorsal horn region (arrows) are shown in C (40x, scale bar = 50 μm).

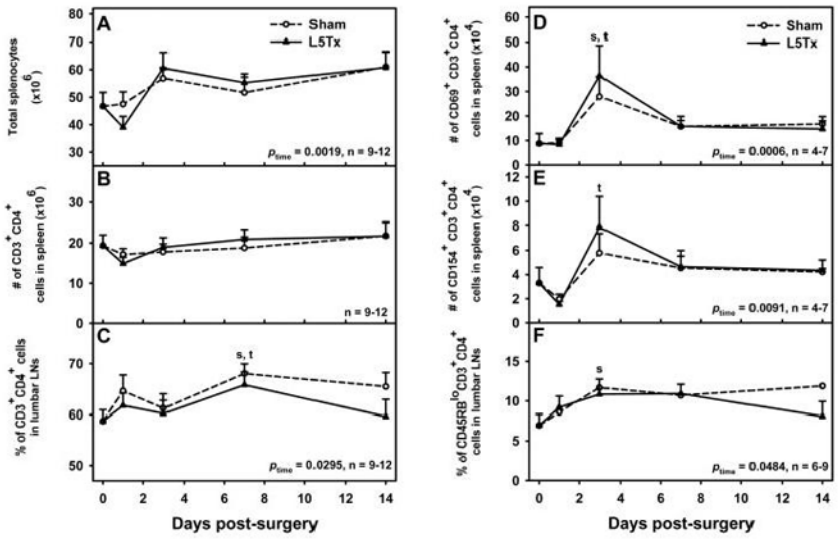

Figure 4. Changes in CD4$^+$ T lymphocytes in the peripheral lymphoid organs post-L5Tx or sham surgery in BALB/c mice

Total cells isolated from spleen and lumbar LNs of sham and L5Tx operated mice were labeled with mAbs and analyzed via FACS. Changes in the numbers of total splenocytes (A), numbers of splenic CD4$^+$ T lymphocytes (CD3$^+$CD4$^+$) (B), and percentage of CD4$^+$ T lymphocytes in the lumbar LNs (C) after surgeries are presented in the left column. Activation of splenic and LNs CD3$^+$CD4$^+$ cells were further determined through their surface expression of CD69, CD154 and CD45RB. Representative data are shown in D–F in the right column. Numbers of animals per group are indicated in each graph. Data are presented as mean ± SEM and "s" or "t" denote significant differences between selected time and day 0 within sham and L5Tx groups, respectively ($p < 0.05$).

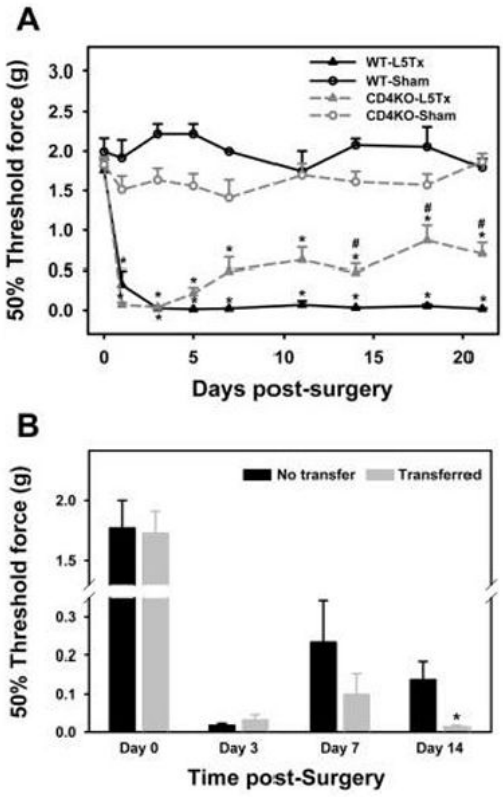

Figure 5. Mechanical sensitivity of CD4KO BALB/c mice post-L5Tx or sham surgery

A: Adult male and female CD4KO BALB/c mice (n = 18 per group) and male BALB/c wild type controls (n = 7 per group) were subjected to L5Tx or sham surgery. Mechanical sensitivity was tested with von Frey filaments using the Up-Down method before and after surgery. Mechanical sensitivity was presented as the 50% threshold force for each animal (mean ± SEM). * indicates significant differences between L5Tx and sham operated mice within CD4KO or wild type groups ($p < 0.05$). # indicates significant differences between CD4KO and wild type mice subjected to the same surgery ($p < 0.05$). B: Mechanical sensitivity is shown in CD4 KO mice (black bar, n = 4) and CD4 KO mice adoptively transferred with $CD4^+$ leukocytes (gray bar, n = 6) subjected to L5Tx at different times after surgery. Results of behavioral tests are presented as described in A. * indicates significant differences between non-transferred group and $CD4^+$ leukocyte transferred group ($p < 0.05$).

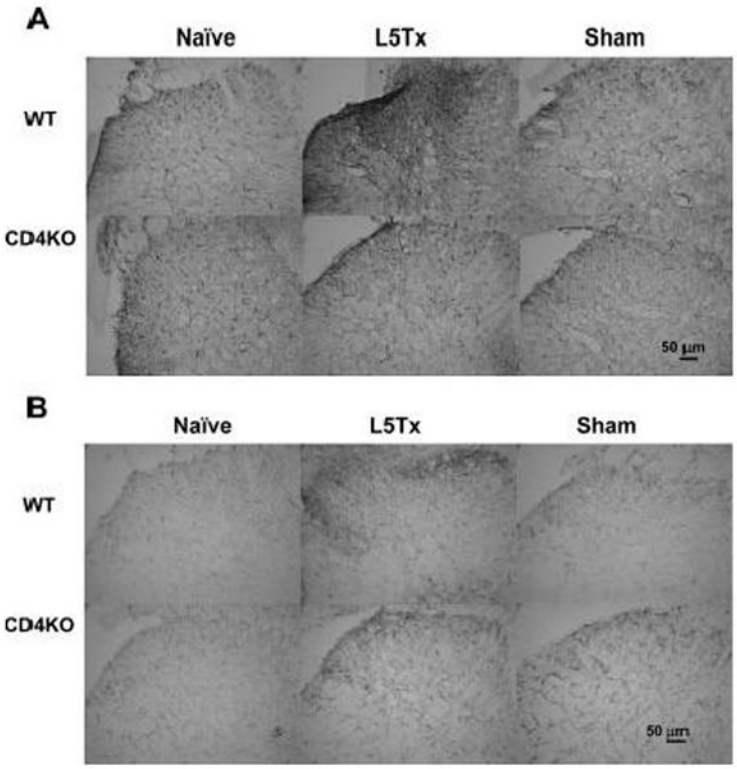

Figure 6. Glial responses in the L5 lumbar spinal cord dorsal horn post-L5Tx or sham surgery in WT and CD4 KO BALB/c mice

L5 lumbar spinal cord sections were prepared from both WT and CD4 KO mice 7 days post-L5Tx or sham surgery and naïve mice (2–3 mice per group). Immunohistochemical staining for GFAP (astrocyte marker, A) and CD11b (microglial marker, B) were performed separately. Representative photomicrographs of the ipsilateral dorsal horn region of L5 lumber spinal cord are shown here (20x, scale bar = 50 μm).

Table 1

Combinations of primary Abs used for FACS

Experiment	Section in text	Primary Ab combination
i) Initial determination of lumbar spinal cord leukocyte infiltration	section 2.2	PE-anti-mouse CD45
ii) Phenotypic analysis of lumbar spinal cord infiltrating and splenic leukocytes	section 2.2 and section 2.3 data not shown	Tube 1) APC-Cy7-anti-mouse CD45, perCP (or PE-Cy7)-anti-mouse CD3, FITC-anti-mouse CD4, PE-anti-mouse CD8; Tube 2) APC-Cy7-anti-mouse CD45, perCP-anti-mouse CD3, FITC-anti-mouse panNK, PE-anti-mouse CD19; Tube 3) APC-Cy7-anti-mouse CD45, perCP-anti-mouse CD3, FITC-anti-mouse CD11b, PE-anti-mouse I-A^d.
iii) Phenotypic analysis of $CD4^+$ T lymphocytes in spleen and lumbar lymph nodes	Section 2.3	Tube 1)APC-Cy7-anti-mouse CD45, PE-Cy7-anti-mouse CD3, FITC-anti-mouse CD4, Biotin-anti-mouse CD45RB; Tube 2)[a] APC-Cy7-anti-mouse CD45, PE-Cy7-anti-mouse CD3, FITC-anti-mouse CD4, PE-anti-mouse CD40L, Biotin-anti-mouse CD69.

[a] for lymph nodes, only tube 1 was used due to the limited numbers of cells available.

All mAbs were from BD Biosciences (San Diego, CA) except that Biotin-anti-mouse CD69 was from eBioscience (San Diego, CA).